Supporting Information

Achieving efficient thick active layer and large area ternary polymer solar cells by incorporating a new fused heptacyclic non-fullerene acceptor

Pan Yin[a], Tao Zheng[a], Yue Wu[b], Gangjian Liu[a], Zhi-Guo Zhang[c], Chaohua Cui*[b], Yongfang Li[bc], and Ping Shen*[a]

[a] Key Laboratory for Green Organic Synthesis and Application of Hunan Province, Key Laboratory of Environmentally Friendly Chemistry and Application of Ministry of Education, College of Chemistry, Xiangtan University, Xiangtan 411105, China

*E-mail: shenping802002@163.com

[b] Laboratory of Advanced Optoelectronic Materials, College of Chemistry, Chemical Engineering and Materials Science, Soochow University, Suzhou 215123, China

*E-mail: cuichaohua@suda.edu.cn

[c] Beijing National Laboratory for Molecular Sciences, CAS Key Laboratory of Organic Solids, Institute of Chemistry, Chinese Academy of Sciences, Beijing 100190, China

Experimental section

Analytical instruments

Nuclear magnetic resonance (NMR) spectra were measured with Bruker AVANCE 400 spectrometer. Ultraviolet-visible (UV-Vis) absorption spectra were measured on PerkinElmer Lamada 25 spectrometer. The photoluminescence (PL) spectrum was conducted on an Edinburgh Instrument FLS 980. Molecular mass was determined by flight mass spectrometry (MALDITOF MS) using a Bruker Aupoflex-III mass spectrometer. Thermal gravimetric analysis (TGA) was performed under nitrogen at a heating rate of 20 °C min^{-1} with TGA Q50 analyzer. Differential scanning calorimetry (DSC) analysis was conducted on a DSC instrument (DSC Q10) in a temperature range from 25 to 320 °C under N_2 with a heating rate of 5 °C min^{-1}. The electrochemical cyclic voltammetry (CV) was recorded

on a electrochemistry work station (CHI830B, Chenhua Shanghai) with a Pt slice electrode (coated with a polymer film), a Pt ring, and an Ag/AgCl electrode as the working electrode, the auxiliary electrode and the reference electrode respectively, in a 0.1 mol L^{-1} tetrabutylammonium hexafluorophosphate (Bu_4NPF_6) acetonitrile solution. X-ray diffraction (XRD) was conducted on X'Pert Pro MPD (PANalytical B.V.) using a CuKα line under room temperature. Atomic force microscopy (AFM) measurement was carried out on a Dimension 3100 (Veeco) Atomic Force Microscope in the tapping mode

Materials

Toluene and tetrahydrofuran (THF) were refluxed and distilled from sodium with benzophenone as an indicator prior to use. *N*, *N*'-Dimethylformamide (DMF) was distilled after drying by CaH_2. *n*-Butyllithium (*n*-BuLi, 2.5 M in THF), lithium diisopropylamide (LDA, 2 M in THF), 1-bromo-4-(hexyloxy)benzene, 3-(dicyanomethylene)indian-1-one, and $Pd(PPh_3)_4$ were purchased from Alfa Aesar or J&K Chemical.

Synthesis of the Target Small Molecule DTCFOIC

The synthetic route of the target non-fullerene acceptor of DTCFOIC was described as **Scheme S1**. The synthetic details of intermediates and target molecule were showed as follows.

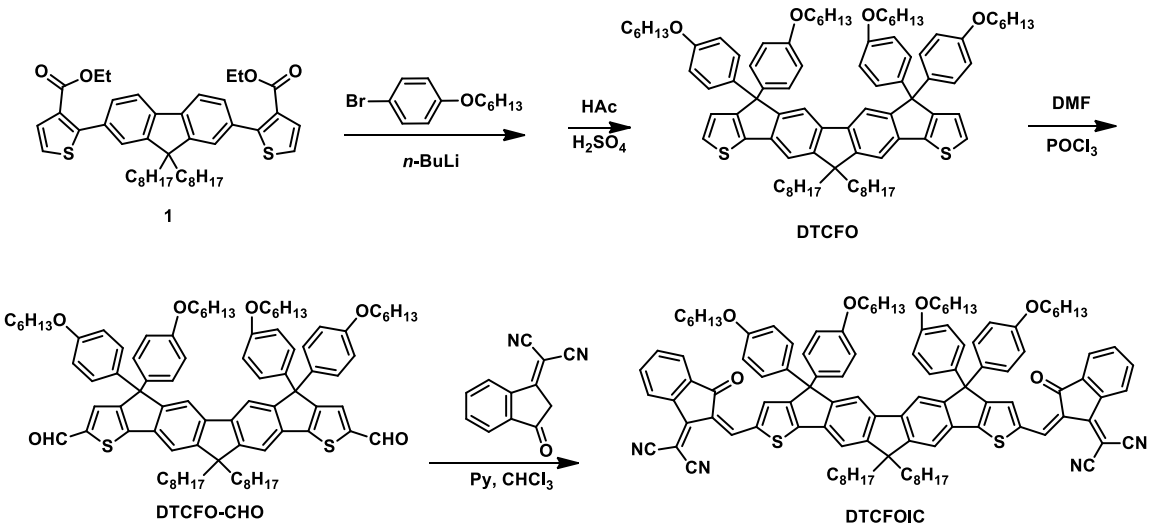

Scheme S1. The synthetic route of DTCFOIC.

Synthesis of DTCFO

To a solution of 1-bromo-4-(hexyloxy)benzene (2.57 g, 20 mmol) in THF (20 mL) was added dropwise a 2.4 M solution of *n*-butyllithium in hexane (6 mL, 15 mmol) at -78°C under nitrogen atmosphere. After being stirred at -78°C for 2 h, compound **1** (1.4 g, 2 mmol) in THF (20 mL) was

added slowly and then stirred overnight at room temperature. The reaction was quenched with water and extracted with CH_2Cl_2 for three times. After the removal of solvent, the crude product was transferred into 250 mL three-neck flask, then acetic acid (40 mL) and concentrated H_2SO_4 (1 mL) were added. Then the mixture was refluxed for 4 h. After cooling to room temperature, the reaction was quenched with water and extracted with ethyl acetate for three times. The combined organic phases were washed with brine three times and dried over anhydrous $MgSO_4$. Finally, the crude product was separated via silica gel column chromatography with petroleum ether/ethyl acetate (50 : 1) as eluent to afford DTCFO as a yellow solid (1.05 g, 40.9%). ^{1}H NMR (400 MHz, $CDCl_3$), δ (ppm): 7.47 (s, 2H), 7.36 (s, 2H), 7.27 (d, J = 8.0 Hz, 2H), 7.15 (d, J = 8.0 Hz, 8H), 6.98 (d, J = 8.0 Hz, 2H), 6.76 (d, J = 8.0 Hz, 8H), 3.89 (t, J = 8.0 Hz, 8H), 1.99 (t, J = 8.0 Hz, 4H), 1.77-1.70 (m, 8H), 1.43-1.40 (m, 8H), 1.32-1.26 (m, 28H), 1.12-1.07 (m, 12H), 0.89 (t, J = 6.0 Hz, 12H), 0.80 (t, J = 6.0 Hz, 6H). ^{13}C NMR (100 MHz, $CDCl_3$), δ (ppm): 157.87, 156.42, 153.15, 150.96, 141.20, 139.21, 137.05, 136.07, 129.09, 127.34, 123.03, 117.19, 114.13, 113.76, 67.86, 61.89, 54.45, 40.66, 31.83, 31.59, 30.13, 29.29, 29.24, 25.76, 23.92, 22.61, 14.10, 14.04. MS (MALDI-TOF, m/z) calcd for $C_{87}H_{110}O_4S_2$: 1283.932; found 1283.461.

Synthesis of DTCFO-CHO

To a dry 100 mL three-necked round bottom flask, compound DTCFO (1.28 g, 1 mmol) and 40 mL of dried DMF was added under a nitrogen atmosphere. The solution was cooled to 0 °C and stirred when 1.5 mL of phosphoryl chloride was added dropwise. The mixture was stirred for 0.5 h at room temperature, and then stirred for 12 h at 100 °C. After cooling to room temperature, the mixture was poured into 20 mL of 1 M NaOH solution and extracted with dichloromethane for three times. The combined organic phases were washed with brine three times and dried over anhydrous $MgSO_4$. Finally, the crude product was purified via silica gel column chromatography with petroleum ether/dichloromethane (4 : 1) as eluent to afford DTCFO-CHO as a yellow solid (0.91 g, 65%). ^{1}H NMR (400 MHz, $CDCl_3$), δ (ppm): 9.83 (s, 2H), 7.63 (s, 2H), 7.53-7.52 (m, 4H), 7.13 (d, J = 8.0 Hz, 8H), 6.78 (d, J = 8.0 Hz, 8H), 3.89 (t, J = 8.0 Hz, 8H), 2.05 (t, J = 8.0 Hz, 4H), 1.77-1.70 (m, 8H), 1.43-1.40 (m, 8H), 1.32-1.26 (m, 28H), 1.12-1.08 (m, 12H), 0.88 (t, J = 6.0 Hz, 12H), 0.78 (t, J = 6.0 Hz, 6H). ^{13}C NMR (100 MHz, $CDCl_3$), δ (ppm): 182.84, 158.26, 156.97, 154.62, 151.98, 151.11, 145.73, 141.19, 135.73, 135.17, 132.00, 128.92, 117.77, 115.61, 114.40, 67.95, 62.15, 54.80, 40.47, 31.78, 31.57, 29.97, 29.25, 29.21, 29.18, 25.74, 23.95, 22.60, 14.07, 14.02. MS (MALDI-TOF, m/z)

calcd for $C_{89}H_{110}O_6S_2$: 1339.952; found 1339.344.

Synthesis of Target Acceptor DTCFOIC

Under nitrogen atmosphere, a mixture solution of compound DTCFO-CHO (804 mg, 0.60 mmol), 3-(dicyanomethylene)indian-1-one (466 mg, 2.40 mmol), pyridine (1 mL), and chloroform (50 mL) was added to a 100 mL round bottom flask and then refluxed for 12 h. After cooling to room temperature, the mixture was poured into methanol (200 mL) and then filtered. The crude product was separated via silica gel column chromatography with petroleum ether/dichloromethane (1 : 1) as eluent to afford DTCFOIC as an aubergine solid (0.46 g, 45.3%). ^{1}H NMR (400 MHz, $CDCl_3$), δ (ppm): 8.90 (s, 2H), 8.69 (d, J = 8.0 Hz, 2H), 7.94 (d, J = 8.0 Hz, 2H), 7.74 (d, J = 8.0 Hz, 4H), 7.67 (d, J = 8.0 Hz, 4H), 7.57 (s, 2H), 7.14 (d, J = 8.0 Hz, 8H), 6.80 (d, J = 8.0 Hz, 8H), 3.90 (t, J = 8.0 Hz, 8H), 2.05 (t, J = 8.0 Hz, 4H), 1.77-1.70 (m, 8H), 1.43-1.40 (m, 8H), 1.32-1.26 (m, 28H), 1.16-1.12 (m, 12H), 0.88 (t, J = 6.0 Hz, 12H), 0.79 (t, J = 6.0 Hz, 6H). ^{13}C NMR (100 MHz, $CDCl_3$), δ (ppm): 188.39, 160.55, 160.11, 158.37, 158.09, 155.91, 152.82, 142.44, 140.76, 139.97, 139.42, 138.55, 136.94, 135.66, 135.37,135.07, 134.40, 128.97, 125.30, 123.72, 121.77, 118.20, 116.53, 114.77, 114.73, 114.53, 68.83, 67.99, 62.19, 54.67, 40.36, 31.78, 31.57, 30.04, 29.27, 29.23, 25.73, 24.14, 22.62, 22.60, 14.09, 14.02. MS (MALDI-TOF, m/z) calcd for $C_{113}H_{118}N_4O_6S_2$: 1692.29; found 1693.881.

PSC Device Preparation and Performance Measurement

The devices with an inverted structure of ITO/ZnO/active layer/MoO_3/Al were fabricated and characterized in an N_2-filled glovebox, where the active layer was of the binary or ternary blends comprised with polymer donor PBDB-T, $PC_{71}BM$ and/or DTCFOIC. The indium tin oxide (ITO) patterned glass was cleaned with ultrasonic treatment in detergent, deionized water, acetone, ethanol, and isopropyl alcohol sequentially, and dried in an ultraviolet–ozone chamber for 15 min. The ZnO layer was deposited by spin-coating on top of a pre-cleaned ITO-coated glass substrate. And then, the active layer was spin-coated on the ZnO layer from a blend solution. The binary and ternary blends were dissolved in chlorobenzene (CB) with different weight ratios. The device was transferred to a glove box, where the above prepared blend solution was then spin-coated on ZnO surface as the active layer. Here, it should be noted that a certain amount of 1,8-diiodooctane (DIO) was added to use as a process additive if necessary. Subsequently, a MoO_3 layer (~10 nm) and an Al layer (~100 nm) were evaporated though a shadow mask and form a top anode. The active area of the devices (~0.04, 0.1, 0.2 or 1.0 cm^2) was defined by a shadow mask. The thicknesses of the active layer were controlled by

varying the spin-coating speed and blend concentration and measured on an Ambios Technology XP-2 surface profilometer. Photovoltaic performance of solar cells was tested under illumination condition with an AM 1.5G (100 mW cm^{-2}), and the current density-voltage (*J*-*V*) characteristics were measured by a computer controlled Keithley 2450 Source Meter. The EQE was measured by using a Solar Cell Spectral Response Measurement System QE-R3011 (Enli Technology Co., Ltd.). The light intensity at each wavelength was calibrated by a standard single-crystal Si solar cell.

The charge mobility was measured by the space charge-limited current (SCLC) method with a hole-only device configuration (ITO/PEDOT:PSS/active layer/MoO_3/Al) for hole mobility and an electron-only device configuration (ITO/ZnO/active layer/Ca/Al) for electron mobility. Both hole and electron mobilities were extracted by fitting measured *J*-*V* curves using the empirical Mott–Gurney formula in single carrier SCLC device with the equation of $ln(JL^3/V^2) \approx 0.89(1/E_0)^{0.5} (V /L) + ln(9\varepsilon_0\varepsilon_r\mu/8)$.

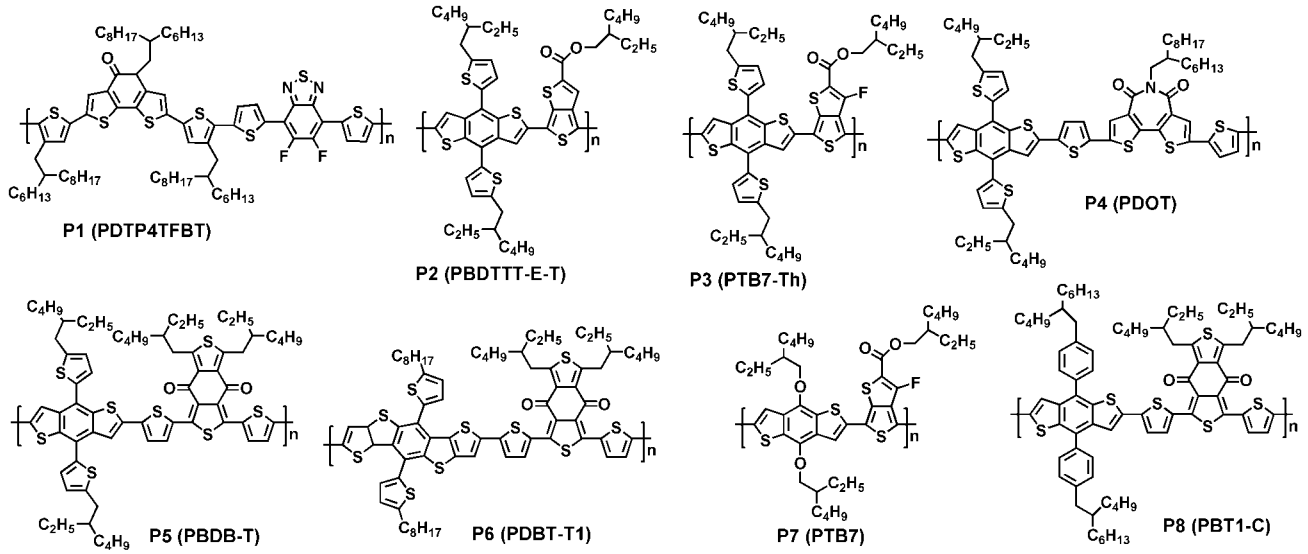

Fig. S1 The chemical structures of the polymer donors of **P1**-**P8** as denoted in Table 1.

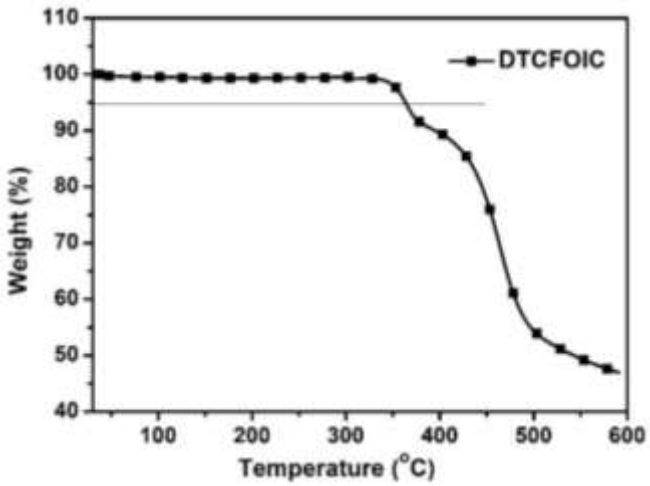

Fig. S2 TGA curve of DTCFOIC under nitrogen atmosphere at a heating rate of 20 °C min^{-1}.

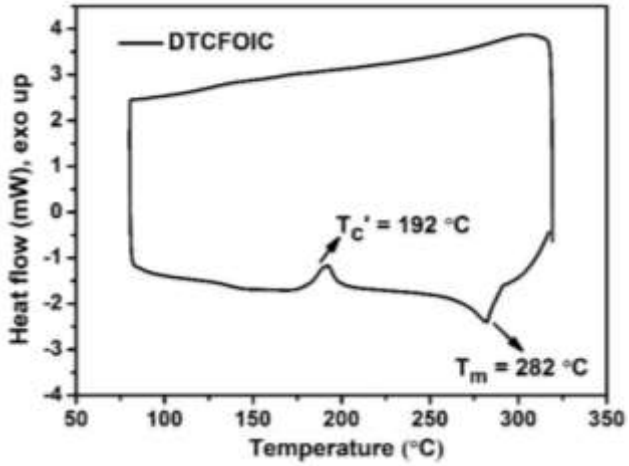

Fig. S3 DSC curve of DTCFOIC under nitrogen atmosphere at a heating rate of 5 °C min^{-1}.

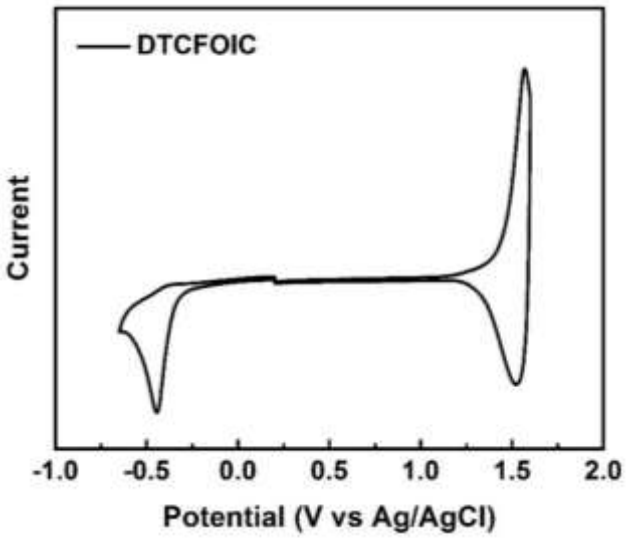

Fig. S4 Cyclic voltammograms of the DTCFOIC film on platinum electrode in acetonitrile solution containing 0.1 mol L^{-1} Bu_4NPF_6 at a scan rate of 0.1 V s^{-1}.

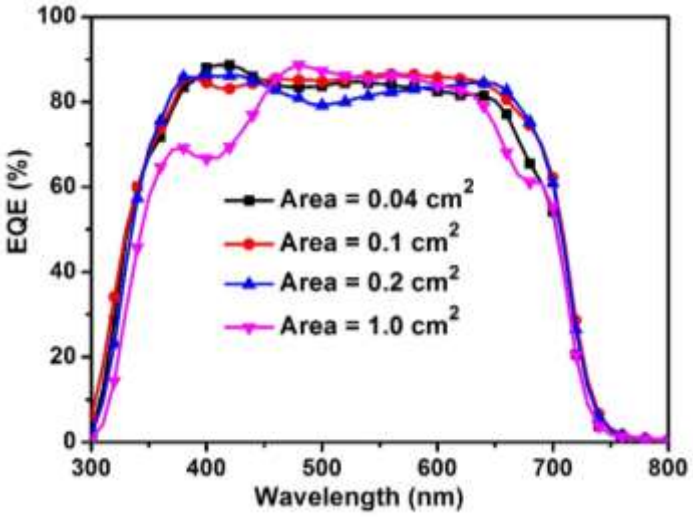

Fig. S5 The EQE plots of the optimal ternary PSCs with the active layer area of 0.04 cm^2 (PCE = 10.13%), 0.1 cm^2 (PCE = 10.41%), 0.2 cm^2 (PCE = 9.14%), and 1.0 cm^2 (PCE = 9.21%).

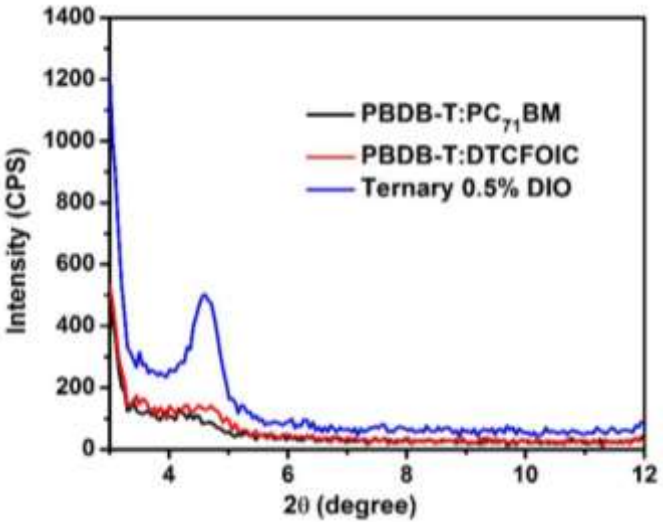

Fig. S6 XRD patterns of the binary PBDB-T:$PC_{71}BM$ and PBDB-T:DTCFOIC, and ternary PBDB-T:$PC_{71}BM$:DTCFOIC blend films.

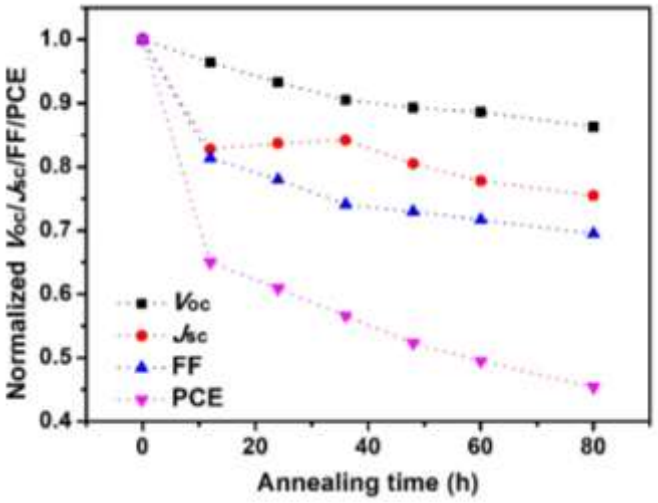

Fig. S7 Changes of normalized V_{oc}, J_{sc}, FF, and PCE of the optimal ternary PSC with different annealing time at 120 °C.

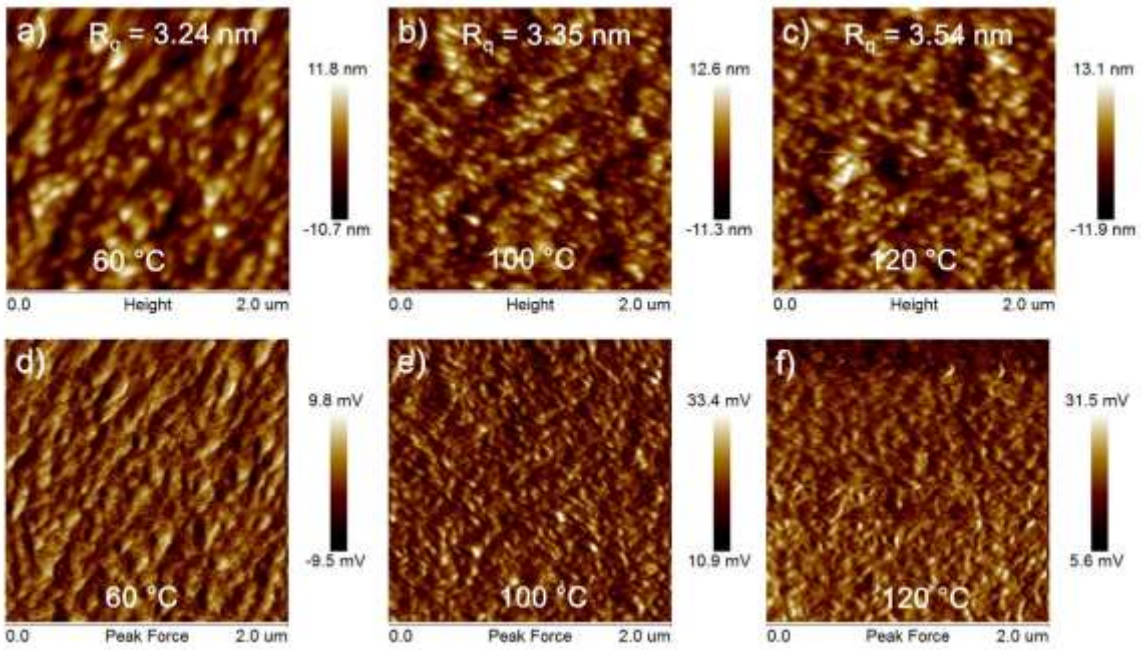

Fig. S8 a-c) AFM height images and d-f) phase images of the optimal ternary blend films exposed at 60, 100, and 150 °C, respectively.

Table S1 Photovoltaic performance of the binary PSCs based on PBDB-T:$PC_{71}BM$ with different fabricated conditions. The devices were in inverted structure of ITO/ZnO/active layer/MoO_3/Al.

PBDB-T:$PC_{71}BM$ [weight ratio]	V_{oc} [V]	J_{sc} [mA cm^{-2}]	FF [%]	PCE [%]	DIO [%]	Area [cm^2]	Thickness [nm]
1:1	0.89	10.28	64.12	5.90	0	0.04	98
1:1.5	0.89	11.40	68.68	6.98	0	0.04	105
1:2	0.88	11.53	61.07	6.22	0	0.04	103
1:1.5	0.82	14.50	58.01	6.92	1	0.04	110
1:1.5	0.82	14.47	56.33	6.65	2	0.04	106

Table S2 Photovoltaic performance of the binary PSCs based on PBDB-T:DTCFOIC with different fabricated conditions. The devices were in inverted structure of ITO/ZnO/active layer/MoO_3/Al.

PBDB-T:DTCFOIC [weight ratio]	V_{oc} [V]	J_{sc} [mA cm^{-2}]	FF [%]	PCE [%]	DIO [%]	Area [cm^2]	Thickness [nm]	Thermal Annealing
1:1	1.07	9.9	53.0	5.61	1	0.04	106	130 °C, 10 min
1:1	1.02	9.3	60.1	5.70	0	0.04	110	no
1:1	1.01	10.3	61.8	6.40	0	0.04	103	130 °C, 10 min
1:1.5	1.00	11.9	57.9	6.92	0	0.04	100	130 °C, 10 min
1:2	0.98	7.88	60.2	4.67	0	0.04	105	130 °C, 10 min

Table S3 Photovoltaic performance of the ternary PSCs based on PBDB-T:PC_{71}BM:DTCFOIC with different feed ratio and DIO content. The devices were in inverted structure of ITO/ZnO/active layer/MoO_3/Al.

PBDB-T:PC_{71}BM:DTCFOIC [weight ratio]	V_{oc} [V]	J_{sc} [mA cm^{-2}]	FF [%]	PCE [%]	DIO [%]	Area [cm^2]	Thickness [nm]
1:1.5:0.1	0.90	12.67	69.7	7.92	0	0.04	95
1:1.5:0.1[a)]	0.83	9.85	46.4	3.78	0	0.04	95
1:0.1:1.5	1.01	7.37	51.7	3.86	0	0.04	85
1:0.1:1.5[a)]	0.98	8.46	55.2	4.58	0	0.04	85
1:1.5:0.2	0.91	13.08	68.3	8.14	0	0.04	90
1:1.5:0.3	0.91	12.29	62.1	6.93	0	0.04	90
1:1.5:0.2	0.85	15.04	66.0	8.61	0.2	0.04	96
1:1.5:0.2	0.87	15.06	67.0	9.40	0.5	0.04	100
1:1.5:0.2	0.88	14.73	67.1	8.73	1	0.04	95
1:1.5:0.2	0.84	14.35	65.8	7.89	2	0.04	93
1:1.5:0.2	0.84	14.60	65.1	7.99	3	0.04	90

[a)] Active layer with thermal annealing treatment at 130 °C for 10 min.

Table S4 Photovoltaic properties of the ternary PSCs based on different active thickness and area with the optimal blend ratio and DIO content.

PBDB-T:$PC_{71}BM$:DTCFOIC [weight ratio]	V_{oc} [V]	J_{sc} [mA cm^{-2}]	FF [%]	$PCE_{max}/_{ave}$[a)] [%]	DIO [%]	Area [cm^2]	Thickness [nm]
1:1.5:0.2	0.86	15.34	67.0	8.90/8.87	0.5	0.04	88
1:1.5:0.2	0.87	15.96	67.0	9.40/9.33	0.5	0.04	100
1:1.5:0.2	0.87	17.43	60.5	9.19/9.15	0.5	0.04	150
1:1.5:0.2	0.87	18.46	63.3	10.13/10.08	0.5	0.04	160
1:1.5:0.2	0.88	17.84	62.0	9.69/9.68	0.5	0.04	180
1:1.5:0.2	0.86	17.27	56.6	8.45/8.44	0.5	0.04	260
1:1.5:0.2	0.87	15.06	66.9	8.81/8.76	0.5	0.1	100
1:1.5:0.2	0.88	16.84	63.8	9.40/9.34	0.5	0.1	110
1:1.5:0.2	0.86	18.55	60.8	9.64/9.62	0.5	0.1	150
1:1.5:0.2	0.88	18.56	64.1	10.41/10.38	0.5	0.1	190
1:1.5:0.2	0.87	18.46	63.3	10.13/10.08	0.5	0.1	200
1:1.5:0.2	0.87	17.98	59.4	9.28/9.22	0.5	0.1	255
1:1.5:0.2	0.86	17.58	57.7	8.67/8.66	0.5	0.1	300
1:1.5:0.2	0.86	15.32	64.4	8.55/8.48	0.5	0.2	103
1:1.5:0.2	0.87	18.22	58.1	9.14/9.12	0.5	0.2	162
1:1.5:0.2	0.85	15.88	60.3	8.16/8.15	0.5	0.2	189
1:1.5:0.2	0.85	15.48	64.0	8.42/8.40	0.5	0.2	206
1:1.5:0.2	0.86	16.50	59.0	8.30/8.26	0.5	0.2	220
1:1.5:0.2	0.87	15.07	66.9	8.81/8.77	0.5	1.0	116
1:1.5:0.2	0.88	14.76	64.7	8.37/8.35	0.5	1.0	132
1:1.5:0.2	0.87	17.49	60.2	9.21/9.18	0.5	1.0	172

[a)] Average PCE values are obtained from over 12 cells fabricated in parallel.

Table S5 Photovoltaic properties of the ternary PSCs with different annealing time at 120 °C with the optimal blend ratio and DIO content.

Annealing time [h]	V_{oc} [V]	J_{sc} [mA cm^{-2}]	FF [%]	PCE [%]	Normalized PCE
0	0.851	17.42	61.87	9.17	1
12	0.820	14.42	50.35	5.96	0.65
24	0.794	14.58	48.23	5.58	0.61
36	0.770	14.66	45.82	5.19	0.57
48	0.760	14.03	45.18	4.80	0.52
60	0.754	13.56	44.36	4.54	0.50
80	0.734	13.16	43.01	4.16	0.45

Table S6 Photovoltaic properties of the ternary PSCs with different annealing temperature with the optimal blend ratio and DIO content.

Device	Temperature [°C]	V_{oc} [V]	J_{sc} [mA cm^{-2}]	FF [%]	PCE [%]	Normalized PCE
Device 1	25(r.t.)	0.844	16.16	62.40	8.51	1
	40	0.830	16.55	61.83	8.50	1
	60	0.831	16.63	60.81	8.40	0.99
	80	0.836	16.40	61.07	8.37	0.98
	100	0.849	14.78	62.26	7.80	0.92
	120	0.828	15.62	54.63	7.07	0.83
	150	0.828	14.74	57.01	6.96	0.82
Device 2	25(r.t.)	0.852	16.99	62.16	9.00	1
	40	0.853	16.04	62.90	8.60	0.96
	60	0.849	15.73	62.7	8.38	0.93
	80	0.859	15.35	63.97	8.44	0.94
	100	0.863	14.56	64.96	8.17	0.91
	120	0.838	14.03	57.97	6.82	0.76
	150	0.828	14.37	54.55	6.49	0.72

	25(r.t.)	0.852	17.16	61.29	8.97	1
	40	0.849	16.89	60.67	8.70	0.97
	60	0.851	16.51	60.65	8.53	0.95
Device 3	80	0.860	16.06	61.74	8.54	0.95
	100	0.865	14.73	64.08	8.17	0.91
	120	0.838	14.27	56.68	6.78	0.76
	150	0.830	14.84	53.25	6.57	0.73
	25(r.t.)	0.833	17.30	60.63	8.75	1
	40	0.839	16.78	61.30	8.64	0.99
	60	0.857	14.79	64.60	8.20	0.94
Device 4	80	0.825	16.98	56.17	7.87	0.90
	100	0.842	16.23	57.48	7.86	0.90
	120	0.821	15.20	54.50	6.81	0.78
	150	0.823	14.82	55.16	6.73	0.77

Table S7 Photovoltaic properties of the optimal ternary PSCs at room temperature with various time.

Time [h]	V_{oc} [V]	J_{sc} [mA cm^{-2}]	FF [%]	PCE [%]	Normalized PCE
0	0.854	17.60	56.80	8.55	1
12	0.847	17.39	54.36	8.00	0.94
24	0.843	17.04	54.66	7.85	0.92
48	0.837	16.67	54.54	7.61	0.89
80	0.839	16.31	53.15	7.27	0.85
160	0.815	15.92	53.38	6.96	0.81
300	0.824	15.60	52.66	6.77	0.79